Behavioral/Systems/Cognitive

Cell Type-Specific Differences in Chloride-Regulatory Mechanisms and $GABA_A$ Receptor-Mediated Inhibition in Rat Substantia Nigra

Alexandra Gulácsi,[1,2]* Christian R. Lee,[3]* Attila Sík,[1,4] Tero Viitanen,[5] Kai Kaila,[5] James M. Tepper,[3] and Tamás F. Freund[1]

[1]Institute of Experimental Medicine, Hungarian Academy of Sciences, Budapest, H-1083 Hungary, [2]Department of Neurobiology, School of Medicine, University of Pittsburgh, Pittsburgh, Pennsylvania 15261, [3]Center for Molecular and Behavioral Neuroscience, Rutgers University, Newark, New Jersey 07102, [4]Centre de Recherche Université Laval Robert-Giffard, Quebec City, Quebec G1J 2G3 Canada, and [5]Department of Biosciences, Division of Animal Physiology, University of Helsinki, Helsinki 00014, Finland

The regulation of intracellular chloride has important roles in neuronal function, especially by setting the magnitude and direction of the Cl^- flux gated by $GABA_A$ receptors. Previous studies have shown that $GABA_A$-mediated inhibition is less effective in dopaminergic than in GABAergic neurons in substantia nigra. We studied whether this phenomenon may be related to a difference in Cl-regulatory mechanisms. Light-microscopic immunocytochemistry revealed that the potassium–chloride cotransporter 2 (KCC2) was localized only in the dendrites of nondopaminergic (primarily GABAergic) neurons in the substantia nigra, whereas the voltage-sensitive chloride channel 2 (ClC-2) was observed only in the dopaminergic neurons of the pars compacta. Electron-microscopic immunogold labeling confirmed that KCC2 is localized in the dendritic plasma membrane of GABAergic neurons close to inhibitory synapses. Confocal microscopy showed that ClC-2 was selectively expressed in the somatic and dendritic cell membranes of the dopaminergic neurons. Gramicidin-perforated-patch recordings revealed that the $GABA_A$ IPSP reversal potential was significantly less negative and had a much smaller hyperpolarizing driving force in dopaminergic than in GABAergic neurons. The $GABA_A$ reversal potential was significantly less negative in bicarbonate-free buffer in dopaminergic but not in GABAergic neurons. The present study suggests that KCC2 is responsible for maintaining the low intracellular Cl^- concentration in nigral GABAergic neurons, whereas a sodium-dependent anion (Cl^-–HCO_3^-) exchanger and ClC-2 are likely to serve this role in dopaminergic neurons. The relatively low efficacy of $GABA_A$-mediated inhibition in nigral dopaminergic neurons compared with nigral GABAergic neurons may be related to their lack of KCC2.

Key words: **substantia nigra; chloride regulation; dopaminergic neurons; GABAergic neurons; potassium–chloride cotransporters; chloride channels**

Introduction

The majority of the inputs to the dopaminergic neurons of the substantia nigra (SN) pars compacta (SNc) and the GABAergic neurons of the SN pars reticulata (SNr) are GABAergic (Grofova, 1975; Ribak et al., 1976; Smith and Bolam, 1989). *In vivo* pharmacological studies have shown that the tonic GABAergic synaptic input to which dopaminergic neurons are subject is mediated predominantly or exclusively by $GABA_A$ receptors (Grace and Bunney, 1985; Tepper et al., 1995; Paladini and Tepper, 1999; Paladini et al., 1999). Similarly, most of the inhibitory inputs to the GABAergic neurons of the SNr act through $GABA_A$ receptors (Precht and Yoshida, 1971; Rick and Lacey, 1994).

Despite the ability of GABA and $GABA_A$ agonists to inhibit both dopaminergic and GABAergic neurons of the SN, the GABAergic neurons of the SNr have been shown to be more sensitive to $GABA_A$ receptor-mediated inhibition than the dopaminergic neurons (MacNeil et al., 1978; Grace and Bunney, 1979, 1985; Waszczak et al., 1980; Celada et al., 1999).

The $GABA_A$ receptor is a ligand-gated anion channel, suggesting that the difference in the efficacy of $GABA_A$ receptor-mediated inhibition in dopaminergic and GABAergic neurons may be attributable to a difference in their chloride-regulatory mechanisms. Recent work has shown that the neuron-specific K^+–Cl^- cotransporter isoform, potassium–chloride cotransporter 2 (KCC2), is responsible for the generation of an inwardly directed Cl^- electrochemical gradient in a large variety of central neurons (Jarolimek et al., 1999; Kakazu et al., 1999; Rivera et al., 1999; DeFazio et al., 2000; Vardi et al., 2000; Vu et al., 2000).

Received May 5, 2003; revised June 24, 2003; accepted July 2, 2003.

This study was supported by the Howard Hughes Medical Institute (T.F.F.), National Institutes of Health (NIH)-NS34865 (J.M.T.), NIH-NS30549 (T.F.F.), and Orszagos Tudomanyos Kutatasi Alap Hungary (T 032251), as well as Grant MOP-53285 from the Canadian Institutes of Health Research (A.S.) and Schizophrenia Axis Research grants [Le Fond de la Recherche en Santé de Québec (FRSQ)] (A.S.). A.S. is an FRSQ scholar. We are grateful to Drs. J. A. Payne and R. Smith for the gifts of antisera against KCC2 and ClC-2, respectively. The help of Gábor Nyiri with the preparation of the illustrations is acknowledged. We also thank K. Lengyel, E. Oszwald, and F. Shah for excellent technical assistance.

*A.G. and C.R.L. contributed equally to this work.

Correspondence should be addressed to Dr. Tamás F. Freund, Institute of Experimental Medicine, Hungarian Academy of Sciences, Budapest 8., Szigony u. 43., H-1083 Hungary. E-mail: freund@koki.hu.

 0270-6474/03/238237-10$15.00/0

KCC2 has a high transport rate and appears to be constitutively active, which makes it a very efficient Cl^--extruding device (for review, see Payne et al., 2003).

The only other transporter capable of Cl^- extrusion that is expressed in neurons is the Na^+-dependent anion (Cl^-–HCO_3^-) exchanger (NDAE) (Romero et al., 2000; Grichtchenko et al., 2001). Because the activity of NDAE depends on intracellular pH, it is much less effective at Cl^- extrusion than K^+–Cl^- cotransport (Kaila, 1994; Schwiening and Boron, 1994).

In addition to transporters, certain Cl^- channels, for example, the inwardly rectifying voltage-gated chloride channel 2 (ClC-2), are likely to play a significant role in the clearance of intracellular chloride (Staley, 1994; Smith et al., 1995; Enz et al., 1999). Unlike transporters, channels are passive devices, which are not capable of maintaining an inwardly directed Cl^- gradient. Expression of ClC-2 mRNA has been reported previously in SNc, but not in SNr (Smith et al., 1995).

Relatively little data are available regarding mechanisms of Cl^- regulation in dopaminergic (Ye, 2000) and nondopaminergic neurons of the SN (Ebihara et al., 1995). In the present study, immunocytochemical labeling of KCC2 and ClC-2 was used to determine the distribution of these proteins in SN dopaminergic and GABAergic neurons, and perforated-patch recordings from both cell types were performed to estimate the reversal potential of $GABA_A$-mediated synaptic responses. The data indicate that, although both neuron types are capable of maintaining an inwardly directed Cl^- gradient, Cl^- extrusion is much less efficient in the dopaminergic than in the GABAergic neurons. This difference is attributable to the absence of KCC2 in the dopaminergic neurons, a unique feature that likely contributes to the relatively low efficacy of $GABA_A$-mediated inhibition in these neurons.

Materials and Methods

Tissue preparation

Fourteen male Wistar rats, weighing 250–300 gm, were deeply anesthetized with Equitesin and perfused through the aortic arch with 0.9% NaCl followed by a fixative solution containing 4% paraformaldehyde (Sigma, Deisenhofen, Germany), 0.05% glutaraldehyde (TAAB Laboratories, Aldermaston, Berkshire, UK), and 15% (v/v%) saturated picric acid (Sigma) in 0.1 M phosphate buffer (PB), pH 7.4. After perfusion, brains were removed, and coronal blocks were dissected from the midbrain; then, 60 μm thin sections were cut from the blocks with a Vibratome (Series 1000; Lancer, St. Louis, MO), washed in 0.1 M PB, and immersed in 30% sucrose (Sigma) overnight. For electron microscopy, sections were freeze thawed over liquid nitrogen to optimize the penetration of immunoreagents. For light microscopy, 0.5% Triton X-100 (Sigma) was used in the buffers to enhance the penetration of the antibodies. PB (0.1 M) and Tris-buffered saline (TBS) (0.05 M; pH 7.4; Sigma) were used for rinsing the sections before incubation in the primary antisera.

Immunocytochemistry

Single immunostaining. Single immunolabeling was applied to localize tyrosine hydroxylase (TH), parvalbumin (PV), KCC2, and ClC-2 proteins. After a 30 min incubation in blocking solution containing 2% bovine serum albumin, primary antisera were used against TH (mouse anti-TH; 1:5000; ETI, Piscataway, NJ), PV (mouse anti-PV; 1:1000; Sigma), ClC-2 (rabbit anti-ClC-2; 1:1000; gift from Dr. R. Smith, University of Colorado Health Sciences Center, Denver, CO) (for specificity, see Sik et al., 2000), or KCC2 (rabbit anti-KCC2; 1:500; gift from Dr. J. Payne, University of California, Davis, School of Medicine, Davis, CA) (for specificity, see Williams et al., 1999) for 48 hr at 4°C. Sections were incubated in biotinylated anti-rabbit or anti-mouse secondary antibody (1:200; Vector Laboratories, Burlingame, CA) for 2 hr at room temperature. After rinses in TBS, the sections were incubated in avidin–biotinylated horseradish peroxidase complex (ABC) (1:400; Vector Laboratories) for 2 hr at room temperature. The immunoperoxidase reaction was performed using Ni^{2+}-intensified 3,3′-diaminobenzidine 4-HCl (DAB) (Sigma) as a chromogen and 0.05% H_2O_2. For preembedding immunogold staining, sections were incubated with 1 nm gold-conjugated anti-rabbit secondary antibody (1:200; Aurion, Wageningen, The Netherlands) for 12 hr at 4°C followed by silver intensification (SE-EM; Aurion). Sections were treated with 1% OsO_4 (40 min), dehydrated in graded ethanol and then in propylene oxide, and embedded in Durcupan ACM (Fluka, Neu-Ulm, Germany). Specimens were examined using light microscopes (Axioscope; Zeiss, Oberkochen, Germany; Provis AX70; Olympus Optical, Tokyo, Japan) and electron microscopes (7100; Hitachi, Tokyo, Japan; Tecnai 12; Philips, Eindhoven, The Netherlands; equipped with MegaView CCD camera).

Double immunostaining. After preembedding immunogold staining against KCC2, sections were incubated in TBS containing the primary antibody against the second antigen (mouse anti-TH; 1:5000; or mouse anti-PV; 1:1000) for 24 hr at 4°C. Sections were then treated with biotinylated anti-mouse secondary antiserum for 2 hr, washed, incubated with ABC for 2 hr at room temperature, and rinsed in TBS. The immunoperoxidase reaction was performed using DAB as above. To differentiate the immunogold and DAB end products, a combination of epipolarization and transmitted light microscopy was used (Provis AX70; Olympus Optical).

Double-immunofluorescence labeling. Sections were washed in TBS and then treated with mixtures of two different antisera [mouse anti-TH (1:5000) was mixed with either rabbit anti-ClC-2 (1:1000) or rabbit anti-KCC2 (1:500)] for 24 hr at 4°C. Immunoreactivities were visualized by processing the sections with fluorescein isothiocyanate-conjugated anti-mouse and carbocyanine 3-conjugated anti-rabbit secondary antibodies (1:50 and 1:500, respectively; Molecular Probes, Eugene, OR). Results of double-fluorescence labeling were analyzed both with fluorescent (Olympus Optical AX70 or Zeiss Axioplan 2) and confocal microscopes (Leica, Nussloch, Germany).

Gramicidin-perforated-patch recordings

Electrophysiological experiments were performed on midbrain slices obtained from young adult male Sprague Dawley rats (4–8 weeks of age; 100–200 gm). All of the procedures were performed with the approval of the Rutgers University Institutional Animal Care and Use Committee and in accordance with the National Institutes of Health Guide to the Care and Use of Laboratory Animals. Animals were deeply anesthetized with 100 mg/kg ketamine intraperitoneally and transcardially perfused with 4–5 ml of ice-cold modified Ringer's solution containing (in mM): 225 sucrose, 2.5 KCl, 0.5 $CaCl_2$, 7 $MgCl_2$, 28 $NaHCO_3$, 1.25 NaH_2PO_4, 7 glucose, 1 ascorbate, and 3 pyruvate and bubbled with 95% O_2–5% CO_2. The brain was quickly removed and trimmed to a block containing the midbrain. Coronal sections (350 μm) were cut in the same medium using a Vibroslice (Campden Instruments, Loughborough, UK). Slices were immediately transferred to normal Ringer's solution containing (in mM): 125 NaCl, 2.5 KCl, 1.25 NaH_2PO_4, 25 $NaHCO_3$, 1 $MgCl_2$, 2 $CaCl_2$, 25 glucose, 1 ascorbate, 3 pyruvate, and 0.4 *myo*-inositol, which was heated to 34°C and continuously bubbled with 95% O_2–5% CO_2 for at least 1 hr before recording. In some experiments, $NaHCO_3$ was omitted from the slice buffer and replaced with (in mM): 20 HEPES, 10 NaCl, and 10 NaOH, and the buffer was bubbled with 100% O_2. Slices were visualized at 40× using infrared differential interference contrast microscopy with an Olympus Optical BX50WI fixed-stage microscope.

Perforated-patch current-clamp recordings were obtained using borosilicate pipettes pulled from 1.5-mm-outer-diameter capillary tubing (World Precision Instruments, Sarasota, FL) using a Narishige (Tokyo, Japan) PP-83 vertical pipette puller that possessed *in vitro* impedances of 5–7 MΩ. The electrodes were filled with a solution containing (in mM): 129 potassium gluconate, 11 KCl, 10 HEPES, 2 $MgCl_2$, 10 EGTA, 3 Na_2-ATP, and 0.3 Na_3-GTP. Gramicidin was dissolved into a stock solution with DMSO and was added to the pipette solution and sonicated just before recording at a concentration of 100 μg/ml. Recordings were amplified by a Neurodata (New York, NY) IR 183 amplifier and displayed on a Tektronix (Beaverton, OR) 511A oscilloscope. The recordings were then digitized by a Nicolet (Madison, WI) 4094C digital oscilloscope and

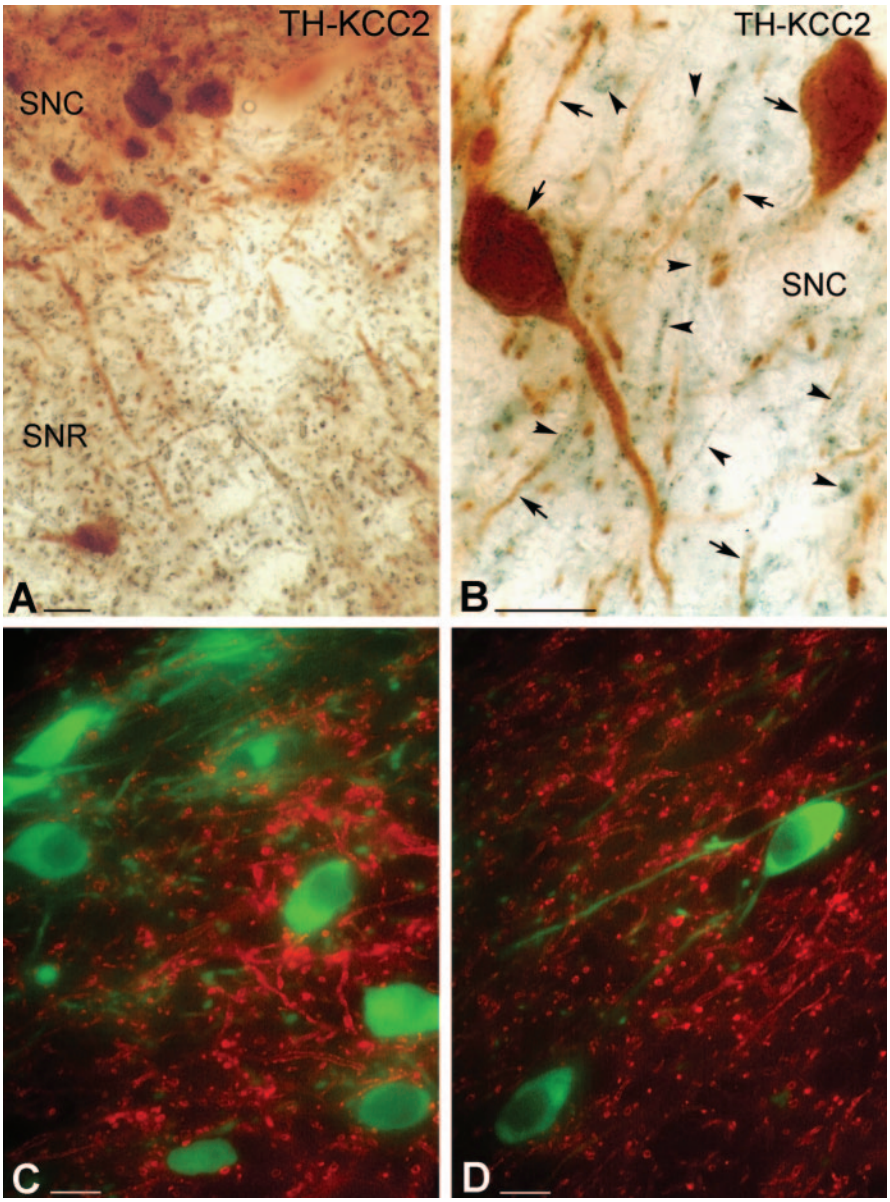

Figure 1. Light micrographs demonstrate the localization of KCC2 in nondopaminergic cells of the rat SN. *A*, *B*, Low (*A*)- and high (*B*)-magnification micrographs illustrate the segregation of TH-immunolabeled neurons (brown) and KCC2-immunopositive dendrites (blue-black) in both the SNc (SNC) and SNr (SNR). Both somata and dendrites of the dopaminergic neurons are labeled for TH (arrows). KCC-2 was found only in the dendritic compartment of nondopaminergic cells (arrowheads). *C*, *D*, Double-immunofluorescent staining shows a mutually exclusive distribution pattern for TH and KCC2. It demonstrates that none of the TH-positive (green) dendrites or somata are outlined by KCC2 immunoreactivity (red). Scale bars, 25 μm.

stored on a Macintosh computer for off-line analysis with custom-designed software.

Stimulating electrodes were constructed from bipolar stainless-steel wires (100 μm diameter; California Fine Wire, Grover Beach, CA). The wires were insulated with enamel except for the tips. For each experiment, the stimulating electrode was placed within the SNr near the ventral border of the nucleus. Single square-wave pulses (0.1–0.5 msec duration) were delivered by a Winston (Millbrae, CA) A-65 timer and SC-100 constant-current stimulus isolation unit delivered at 0.75 Hz.

Current–voltage relationships were measured from 500 msec hyperpolarizing pulses from the resting membrane potential. Reversal potentials were determined by measuring the voltage change in the recorded neuron in response to stimulation of the SNr at various membrane potentials produced by either steady-state current or 600 msec hyperpolarizing pulses delivered from the resting membrane potential. The contribution of $GABA_A$ receptor-mediated currents to the postsynaptic potential was isolated by recording in the presence of the competitive non-NMDA glutamate receptor antagonist 6-cyano-7-nitroquinoxalene-2,3,-dione (10 μM), the $GABA_B$ receptor antagonist CGP 35348 (200 μM), and either 2-amino-5-phosphonopentanoic acid (50 μM) or ketamine (100 μM), which are both NMDA receptor antagonists. In some cases, bicuculline (50 μM) was added to the above solution to further confirm the identity of the postsynaptic potential being measured.

Neurons were classified as either dopaminergic or GABAergic on the basis of their electrophysiological properties. The presence of a slowly developing sag in the voltage deflection in response to hyperpolarizing current injection, which is the result of activation of an H-current, and the presence of slow spontaneous firing with wide spikes (>2 msec) with large-amplitude, long-duration spike afterhyperpolarizations were the defining characteristics of dopaminergic neurons (Kita et al., 1986; Grace and Onn, 1989; Richards et al., 1997; Iribe et al., 1999). The GABAergic neurons of the SNr were identified by their narrower spikes, shorter spike afterhyperpolarization, higher firing rate, and lack of H-current (Nakanishi et al., 1987; Richards et al., 1997).

Reversal potentials were determined from the zero voltage intercept of the linear regression of the peak postsynaptic potential amplitude versus the membrane potential (Iribe et al., 1999). All of the potentials were corrected for the measured junction potential (13 mV in normal Ringer's and 11 mV in bicarbonate-free buffer). The reversal potentials were compared using two-tailed Student's *t* tests. All of the results are presented as mean ± SEM.

Results

KCC2 is localized in GABAergic but not in dopaminergic neurons of the SN: light-microscopic studies

Immunoperoxidase labeling revealed that KCC2 protein was localized mostly in dendrites but not in axon terminals of neurons in the SN (Fig. 1*A*,*B*). The somatic plasma membrane of neurons with densely positive dendrites was labeled only very faintly, and these somata were restricted to pars reticulata. Glial cells were completely devoid of KCC2 immunostaining. Double-labeling experiments were performed to reveal the neurochemical identity of the KCC2-immunoreactive neurons (Fig. 1). First, the expression pattern of KCC2 was investigated in dopaminergic neurons using two different double-labeling methods. Dopaminergic cells were identified on the basis of their TH expression (Isaacs and Jacobowitz, 1994). Double-immunofluorescent staining clearly demonstrated that none of the TH-positive dendrites or somata were outlined by KCC2 immunoreactivity; the two staining patterns were mutually exclusive (Fig. 1*C*,*D*). In another set of experiments, TH was visualized by immunoperoxidase staining using DAB as a chromogen, whereas KCC2 was revealed by DAB-Ni (Fig. 1*A*,*B*) or preembedding immunogold labeling with silver enhancement (not shown). In agreement with the results of fluorescent double staining, DAB-Ni or immunogold (KCC2) label-

ing was found in the dendritic compartment of only nondopaminergic (i.e., TH-negative) neurons. Thus, TH-positive dendrites and KCC2-immunoreactive dendrites formed two distinct populations in both the SNc and SNr (Fig 1).

To demonstrate the presence of KCC2 in GABAergic neurons, a subset of GABAergic neurons was identified by PV immunoreactivity using DAB as chromogen coupled with preembedding immunogold staining for KCC2 (Fig. 2). Parvalbumin has been shown previously to be present in GABAergic but not in dopaminergic neurons in the SN (Rajakumar et al., 1994; McRitchie et al., 1996; Hontanilla et al., 1997). The present results confirmed that, unlike dopaminergic cells, GABAergic neurons do express KCC2 protein (Fig. 2).

These findings raised the possibility that dendrites of TH-positive neurons also contain KCC2, but that its expression is masked by DAB end product when using conventional light-microscopic methods. Therefore, the KCC2–TH double-staining (using immunogold and DAB) was repeated, and epipolarization microscopy was used to avoid false-negative results. This technique has the advantage of separating light-scattering immunogold particles from DAB immunostaining, allowing the detection of two different immunoreaction end products separately in the same double-immunolabeled profiles. Transmitted light microscopy depicted the DAB-stained dopaminergic neurons in the SNc, whereas epipolarization light microscopy demonstrated the KCC2-containing profiles. The results clearly showed that, indeed, KCC2 immunoreactivity was absent from dopaminergic neurons. However, the same epipolarization technique strengthened the positive results that were obtained for KCC2–PV colocalization using conventional light microscopy (Fig. 2).

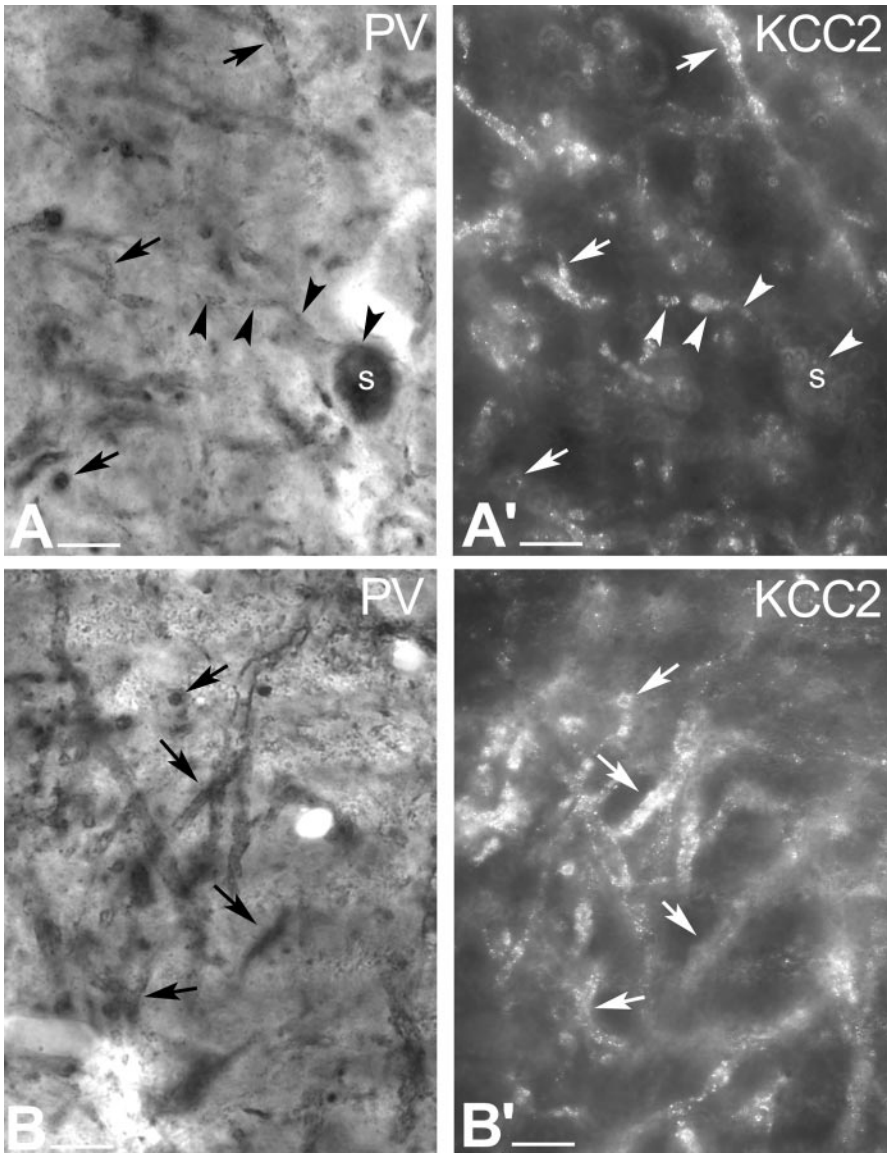

Figure 2. Conventional and epipolarization light micrographs show that, unlike dopaminergic cells, GABAergic neurons express KCC2 protein. *A*, Conventional light-microscopic image illustrates PV-immunopositive profiles in the rat SNr. PV exclusively labels a subset of GABAergic neurons in the SN. Black arrows indicate PV-immunopositive dendrites, whereas black arrowheads outline a PV-immunoreactive neuron with its labeled dendrite. *A′*, In the same section, epipolarization light microscopy illustrates KCC2-immunopositive dendrites. White arrowheads indicate a PV-immunopositive cell, of which only the dendrite but not the soma shows KCC2 immunoreactivity. White arrows show the PV-immunolabeled dendrites, which are also KCC2 immunoreactive. *B*, *B′*, Another example of conventional and epipolarization microscopy showing localization of KCC2 (*B′*) to PV^+, nondopaminergic neurons (*B*). Scale bars, 20 μm. s, Soma.

Subcellular distribution of KCC2-immunoreactive profiles in nondopaminergic neurons: electron-microscopic studies

To reconfirm the absence of KCC2 immunoreactivity in dopaminergic neurons observed at the light-microscopic level, double-immunolabeled sections for KCC2 and TH were analyzed by electron microscopy (Fig. 3). The subcellular localization of KCC2 was revealed using a preembedding immunogold reaction, whereas TH-immunoreactive cells were visualized using DAB as the chromogen. The advantage of immunogold labeling over the immunoperoxidase–DAB method is that the former reaction product is not diffusible; thus, it precisely shows the subcellular localization of the investigated antigen. Immunoreactivity for TH was found in the perikarya and dendrites of the dopaminergic neurons (Fig. 3). In contrast, silver-enhanced gold particles, indicating the presence of KCC2, were localized to the plasma membrane of dendrites of the TH-negative, nondopaminergic neurons ($n = 42$) (Fig. 3). KCC2 immunolabeling in these cells was often seen at the periphery of symmetrical (presumed GABAergic) synapses at the postsynaptic site (Fig. 3*B*). Transport vesicles immunoreactive for KCC2 were occasionally observed in the cytoplasm of TH-immunonegative dendrites (Fig. 3).

On the basis of the light-microscopic observations, PV-immunoreactive neurons were expected to express KCC2 protein. Parvalbumin was used as a neurochemical marker to identify the GABAergic subpopulation of SNr neurons. Double-labeling experiments were performed to investigate colocalization of PV (immunoperoxidase; DAB) and KCC2 (immunogold) in the same profiles (Fig. 4). Immunoreactivity for PV was found in the perikarya (not shown) and

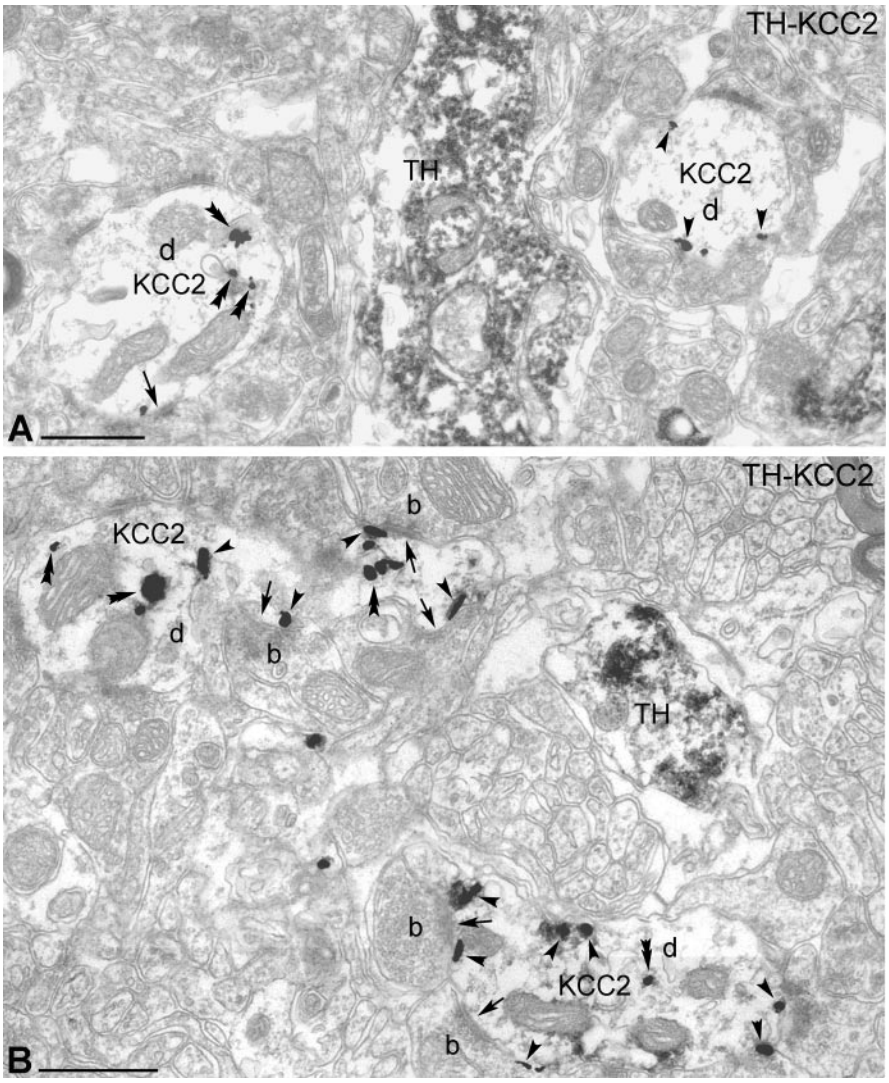

Figure 3. Electron-microscopic localization of KCC2 protein in the rat SN. *A*, *B*, Electron microscopy revealed that TH-immunopositive dendrites (DAB labeled) do not contain KCC2 protein (gold particles). Immunoreactivity for TH was found in dopaminergic dendrites, whereas KCC2 was localized in the dendritic membrane of nondopaminergic neurons. KCC2 immunolabeling (arrowheads) was often observed in the vicinity of symmetric synapses (arrows) at the postsynaptic site. Scale bars, 500 nm. b, Bouton; d, dendrite.

proximal as well as distal dendrites of numerous neurons in the SNr. The vast majority of the PV-immunolabeled cells in the SNr were found to display KCC2 immunoreactivity at the electron-microscopic level. Silver-intensified gold particles were attached to the plasma membrane in the immediate vicinity of symmetric synapses formed by presumed GABAergic inhibitory axon terminals ($n = 65$) (Fig. 4), but were also found, although less frequently, adjacent to asymmetric, presumed excitatory synapses ($n = 23$).

ClC-2 is localized in dopaminergic cells of the SNc

A previous study using *in situ* hybridization demonstrated the presence of ClC-2 mRNA in the SNc (Smith et al., 1995). To investigate whether ClC-2 protein has an identical distribution in the SNc, we used immunocytochemical techniques with DAB as a chromogen. Intensely labeled neurons were observed in the SNc, corresponding to the area in which most dopaminergic cells are normally situated (Fig. 5*A*), but not in the SNr, in which GABAergic cells are located. Light microscopy at high power revealed that ClC-2 immunoreactivity was present not only in the perikarya but also in proximal and distal dendrites of the SNc neurons (Fig. 5*B*). Axon terminals or glial cells were not immunolabeled. The distribution pattern of ClC-2-immunoreactivity strongly suggested that dopaminergic neurons express this type of Cl^- channel. To provide direct evidence, double immunocytochemical analysis was performed, using an antibody against TH to visualize dopaminergic neurons together with ClC-2. The sections were analyzed by using a fluorescent light microscope and a confocal microscope (Fig. 6). ClC-2 immunolabeling was observed in the perikarya and proximal dendrites of most, if not all, of the TH-immunoreactive SNc neurons (Fig. 6*A*,*B*), and all of the ClC-2-positive cells expressed TH immunoreactivity.

Reversal potential and driving force of IPSPs in dopaminergic and GABAergic neurons

Neurons recorded in substantia nigra with gramicidin-perforated patch were identified as dopaminergic ($n = 17$) or principal GABAergic ($n = 19$) neurons on the basis of well established electrophysiological characteristics, including spontaneous firing rate, action potential waveform, spike afterhyperpolarization, and the presence of a slowly developing sag in the response to hyperpolarizing current injection because of I_h (Kita et al., 1986; Nakanishi et al., 1987; Grace and Onn, 1989). These distinguishing properties are illustrated for two representative neurons in Figure 7. Most dopaminergic neurons and all of the GABAergic neurons were spontaneously active at rest. As shown in Figure 7, *A1*, *A2*, *B1*, and *B2*, dopaminergic neurons have slower firing rates, wider duration action potentials, and larger amplitude and longer duration spike afterhyperpolarizations than do GABAergic neurons. In addition, a slowly developing sag in the response to hyperpolarizing current injection attributable to the activation of a slow hyperpolarization-activated cation current (I_h) and an inward rectification was clearly visible in dopaminergic neurons (Fig. 7*A3*,*4*) but was absent from the GABAergic neurons, which displayed a mostly linear current–voltage relation (*B3*,*4*).

Electrical stimulation of the SNr (0.5 msec; 1–5 mA) in the presence of glutamate and $GABA_B$ antagonists (see Materials and Methods) produced IPSPs with latencies to peak of 11.36 ± 0.68 msec in dopaminergic neurons and 10.23 ± 1.28 msec in GABAergic neurons. These IPSPs were completely blocked by 50 μM bicuculline, verifying that they were $GABA_A$ mediated (data not shown).

Figure 8 shows current-clamp recordings from a representative dopaminergic and a representative GABAergic neuron demonstrating changes in the amplitude of the IPSP elicited at different membrane potentials in response to electrical stimulation of the SNr. As shown in Figure 9, the $GABA_A$ IPSP reversal potential

(E_{IPSP-A}) was significantly less hyperpolarizing in dopaminergic neurons (-63.45 ± 2.02 mV) than in GABAergic neurons (-71.58 ± 1.37 mV; $t = 3.20$; df = 22; $p < 0.01$,).

The GABAergic and dopaminergic neurons are spontaneously active, and the latter exhibit subthreshold oscillations caused by the interaction of a persistent low-threshold Ca^{2+} current and a Ca^{2+}-activated K^+ current (Kang and Kitai, 1993a,b; Wilson and Callaway, 2000). Hence, an estimate of the $GABA_A$ IPSP driving force (DF_{IPSP-A}) was calculated as follows: $DF_{IPSP-A} = V_M - E_{IPSP-A}$, where V_M was defined as the most negative value of the membrane potential observed under zero-current conditions (usually the minimum value of the spontaneous spike afterhyperpolarization). This provided estimates of 3.3 ± 2.0 mV ($n = 10$) and 9.5 ± 2.2 mV ($n = 11$) for the DF_{IPSP-A} for dopaminergic and GABAergic neurons, respectively (Fig. 9). These data clearly demonstrate a DF_{IPSP-A} that drives a hyperpolarizing Cl^- current in both cell types, because the present method will, if anything, lead to an underestimate of the amplitude of a driving force with this polarity.

The above experiments indicate that both the GABAergic as well as the dopaminergic neurons must have an active chloride extrusion mechanism capable of maintaining an inwardly directed Cl^- electrochemical gradient. In the GABAergic neurons, Cl^- extrusion is likely to be mediated by KCC2, which we showed is expressed abundantly in these cells. However, the presence of ClC-2 channels in the dopaminergic neurons does not explain their hyperpolarizing $GABA_A$ response, because, although a channel can help in the clearance of an intracellular Cl^- load, it is unable to create a driving force for Cl^-. In light of what is known about neuronal Cl^- extrusion, a likely candidate here is the NDAE (Kaila, 1994; Payne et al., 2003). Hence, we repeated the experiments in bicarbonate-free (HEPES-buffered) solution, to eliminate the activity of the NDAE. These experiments revealed that E_{IPSP-A} in dopaminergic neurons recorded in bicarbonate-free buffer was significantly more depolarized than E_{IPSP-A} in dopaminergic neurons recorded in normal ringers (-49.73 ± 3.16 mV vs -63.45 ± 2.02 mV; $t = 3.38$; df = 15; $p < 0.01$), as shown in Figure 8. In sharp contrast, the E_{IPSP-A} in GABAergic neurons recorded in these two buffers did not differ (-73.41 ± 2.33 mV vs -71.58 ± 1.37 mV). As was the case in normal slice buffer, E_{IPSP-A} was significantly more depolarized in dopaminergic neurons than in GABAergic neurons ($t = 5.94$; $p < 0.01$; df = 10). In addition, the polarity of DF_{IPSP-A} was changed from a positive to a negative value (-12.1 ± 1.9 mV; $n = 4$) in the dopaminergic cells in the absence of bicarbonate, whereas no obvious change in DF_{IPSP-A} in the GABAergic neurons (9.25 ± 2.9 mV; $n = 7$) was seen, as shown in Figure 9.

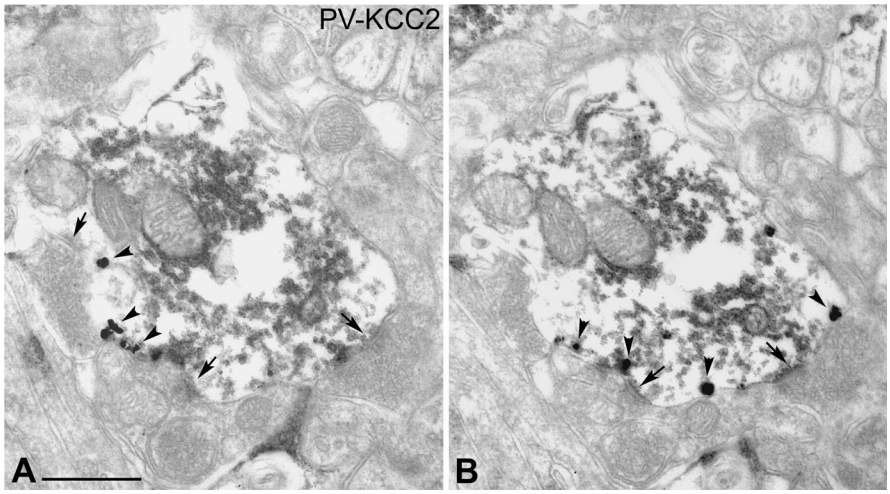

Figure 4. Parvalbumin-immunoreactive neurons express KCC2 in the rat SN. *A*, *B*, Electron micrographs taken from two consecutive sections demonstrate the presence of KCC2 (gold particles) in the PV-immunopositive (DAB-labeled) dendrites. Gold particles show that KCC2 is often localized near to the symmetric synapses (arrows). Arrowheads indicate gold particles. Scale bar: (in *A*) *A*, *B*, 500 nm.

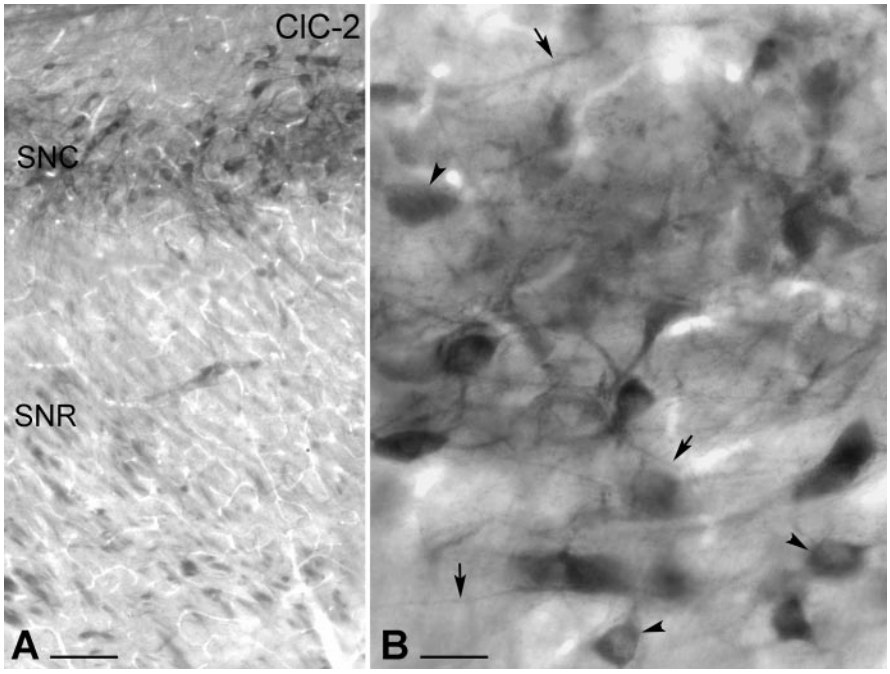

Figure 5. Light-microscopic illustration of the distribution of ClC-2-immunolabeled neurons in the rat SN. *A*, Low-magnification light micrograph shows the presence of ClC-2-immunopositive cells in the SNc (SNC). ClC-2-immunopositive cells were visualized by immunoperoxidase reaction (DAB; black end product). The SNr (SNR) did not display ClC-2 immunoreactivity. *B*, High-magnification micrograph demonstrates that ClC-2 is present not only in the perikarya (arrowheads) but also in distal dendrites of the SNc neurons (arrows). Scale bars: *A*, 100 μm; *B*, 25 μm.

Discussion

The main anatomical findings of the present study indicated that two key molecules involved in neuronal Cl^- homeostasis show a distinct neuron type-specific expression pattern in the rat SN: GABAergic neurons in the SNr express the neuron-specific K–Cl cotransporter KCC2, whereas dopaminergic neurons in the SN are devoid of KCC2 but express ClC-2. Consistent with these results, GABAergic SN neurons were

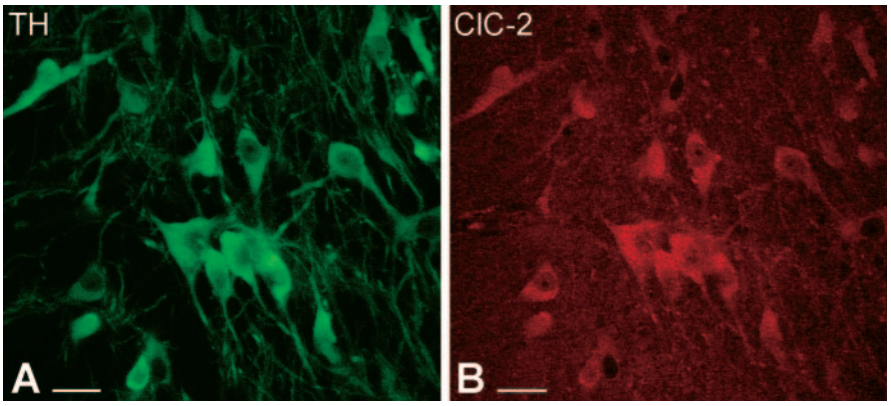

Figure 6. Confocal microscopic images of double-immunostained sections show that TH-immunoreactive dopaminergic neurons express ClC-2 in the SNc. *A*, Immunofluorescence staining against TH visualizes the dopaminergic neurons in the SNc (green). Both perikarya and dendrites display TH immunoreactivity. *B*, In the same section, ClC-2-immunopositive cells were identified on the basis of the presence of a red fluorescent signal. Similarly, immunolabeling was observed selectively in perikarya and proximal dendrites of dopaminergic neurons. Scale bars, 25 μm.

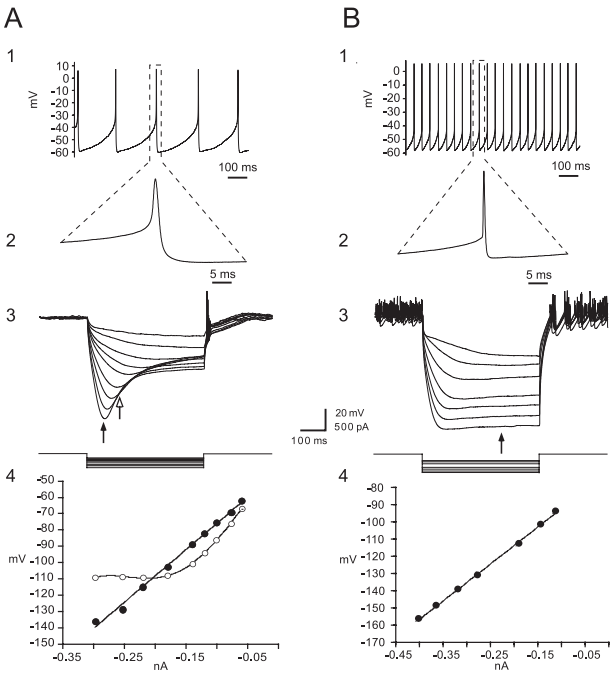

Figure 7. Identification of principal dopaminergic and GABAergic neurons in substantia nigra from current-clamp recordings. *A1*, *A2*, Dopaminergic neurons exhibit slow pacemaker-like firing with broad action potentials exceeding 2.5 msec in duration and a large-amplitude, long-duration spike afterhyperpolarization. *A3*, Dopaminergic neurons exhibit a prominent time-dependent sag in the voltage deflection in response to hyperpolarizing current injection because of a slowly activating I_h. *A4*, *I–V* plots both before (filled circles) and during (open circles) activation of I_h, calculated at the times indicated by the filled and open arrows in *A3* above. The *I–V* relationship was best fit by linear regression before activation of I_h but showed a pronounced inward rectification after its activation, which was best fit by a fourth-power polynomial. *B1*, *B2*, In contrast to dopaminergic neurons, pars reticulata principal GABAergic neurons fire spontaneously at higher rates, have a shorter-duration action potential of ~1 msec in duration, and do not exhibit a prominent large-amplitude spike afterhyperpolarization. *B3*, *B4*, Principal GABAergic neurons lack I_h, and the *I–V* plot, calculated at the time indicated by the arrow, is best fit by linear regression (*B4*). In both cases, the hyperpolarizing current was applied from rest. Traces in *A3* and *B3* are the digital averages of four consecutive single sweeps.

found to exhibit a significantly more hyperpolarized reversal potential for $GABA_A$-mediated synaptic responses than the dopaminergic neurons. As will be discussed below, these observations provide a coherent view on the ionic mechanisms regulating $GABA_A$-mediated hyperpolarizing IPSPs in these two cell types.

Dopaminergic neurons in the SNc express ClC-2 but not KCC2

Expression of ClC-2 mRNA was demonstrated previously in the SNc but not in the SNr using *in situ* hybridization (Smith et al., 1995). In line with this result, we found that ClC-2 protein is exclusively expressed in SN by the dopaminergic neurons. Cl^- flux across ClC-2 channels is rectifying and takes place at relatively negative membrane potentials, which suggests that ClC-2 is involved in the clearance of intracellular Cl^- loads (Smith et al., 1995; Enz et al., 1999). ClC-2 is expressed in retinal rod bipolar cells (Enz et al., 1999) and in hippocampal pyramidal cells (Misgeld et al., 1986; Staley, 1994; Smith et al., 1995; Sik et al., 2000), but its expression cannot explain the hyperpolarizing $GABA_A$ responses observed in these cells, because channel-mediated fluxes are driven by electrochemical ion gradients, but, obviously, they do not generate such gradients. However, bipolar cells as well as hippocampal neurons are known to express KCC2 (Payne et al., 1996; Rivera et al., 1999; DeFazio et al., 2000; Vardi et al., 2000; Vu et al., 2000; Gulyas et al., 2001), which maintains intracellular Cl^- levels at a low level and accounts for hyperpolarizing $GABA_A$ responses in these neurons. In contrast to this, nigral dopaminergic neurons are devoid of KCC2, and the present electrophysiological data suggest that hyperpolarizing $GABA_A$ inhibition in these cells is based on the operation of the NDAE.

GABAergic neurons in the SN express KCC2 but not ClC-2

Our light- and electron-microscopic immunocytochemical localization studies indicate that only nondopaminergic (i.e., presumably GABAergic) neurons express KCC2 protein in the SN. However, a recent study using *in situ* hybridization reported expression of KCC2 both in the SNc and the SNr (Kanaka et al., 2001), but the neurochemical identity of the cells expressing KCC2 mRNA was not determined. Our results suggest that all of the KCC2 mRNA-expressing cells in that study may have been GABAergic cells even in the SNc, because several studies suggest the presence of at lease some GABAergic neurons in this region (Javoy-Agid et al., 1981; Lacey et al., 1989; Hebb and Robertson, 2000). However, even if KCC2 mRNA were present in SNc dopaminergic neurons, it does not necessarily contradict our findings, because the translation to KCC2 protein might be blocked. More importantly, the present electrophysiological findings are completely consistent with our anatomical findings, both arguing strongly against the presence of functional KCC2 in SNc dopaminergic neurons.

That KCC2 has a pivotal role in maintaining low $[Cl^-]_i$ has been demonstrated in different regions and neurons of the rat brain, including the hippocampus, neocortex, and lateral superior olive (Kakazu et al., 1999; Rivera et al., 1999; DeFazio et al., 2000). Although previous electrophysiological data predicted the presence of an active Cl^- extrusion mechanism in the SNr (Ebihara et al., 1995), the transporter involved was not identified. Our anatomical data strongly suggest that KCC2 has a major role in maintaining low Cl^- concentration in GABAergic but not in dopaminergic neurons in substantia nigra.

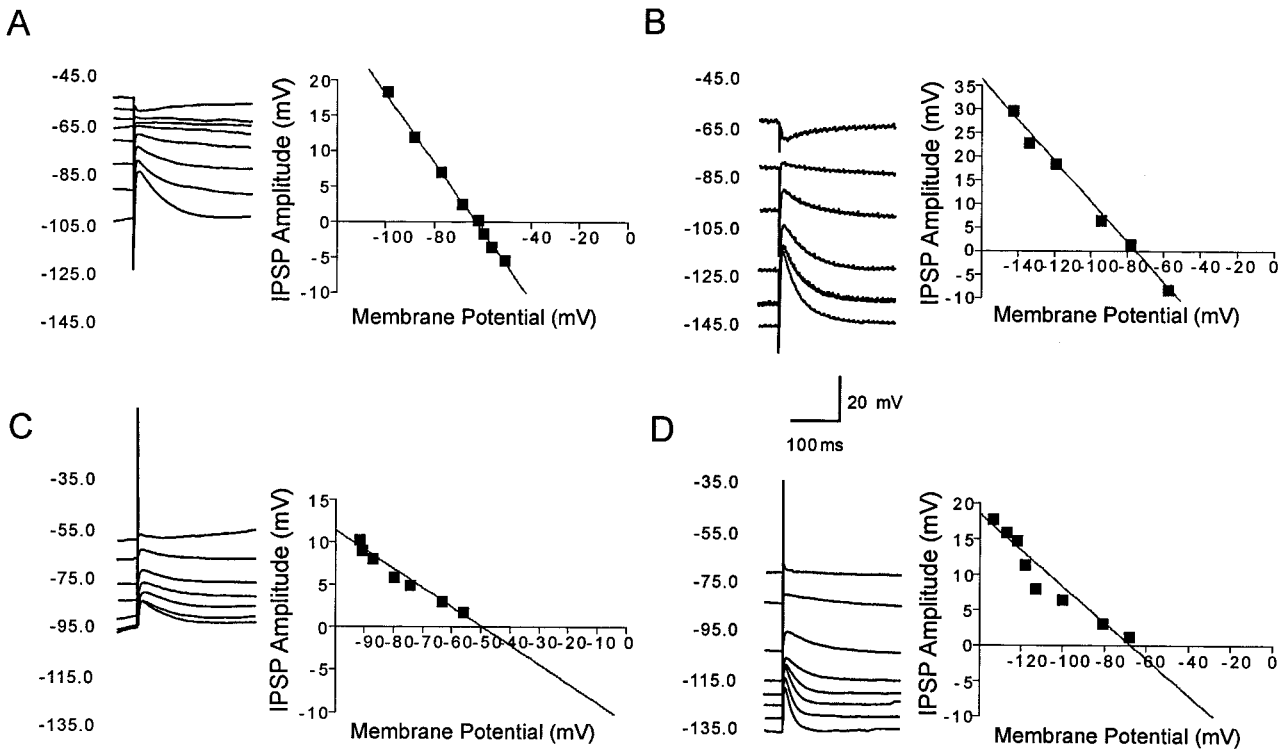

Figure 8. Pharmacologically isolated $GABA_A$ receptor-mediated IPSPs in response to stimulation of the SNr *in vitro*. *A*, Representative current-clamp recordings of a dopaminergic neuron at various membrane potentials show an IPSP in response to stimulation of the SNr. Inset is a plot of the IPSP amplitude versus the membrane potential. The plot of the regression line revealed that the reversal potential of the IPSP was −62.9 mV. *B*, Representative current-clamp recordings of IPSP in GABAergic SNr neuron shows significantly more hyperpolarized reversal potential of −75.6 mV. *C*, *D*, In bicarbonate ion-free slice buffer, the $GABA_A$ receptor-mediated IPSP reversal potential in a representative dopaminergic neuron (*C*) becomes significantly less hyperpolarized at −49.3 mV, whereas there is no significant change in a nondopaminergic neuron in which the IPSP reverses at −67.7 mV (*D*). Each of the traces is an average of four sweeps.

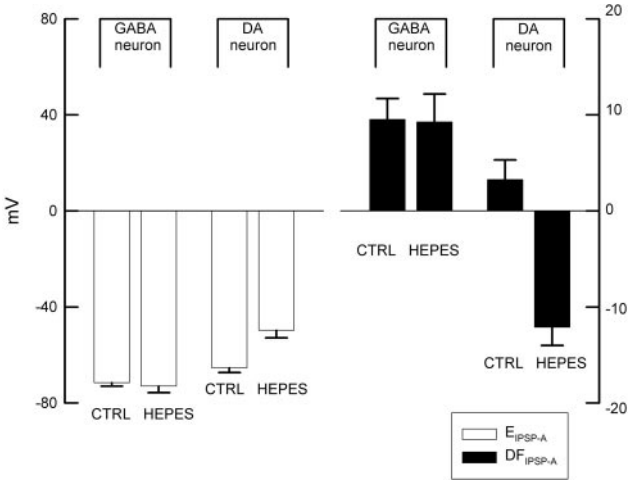

Figure 9. A summary of values for the $GABA_A$ IPSP reversal potential ($E_{IPSP\text{-}A}$) and the $GABA_A$ IPSP driving force ($DF_{IPSP\text{-}A}$) in GABAergic and dopaminergic (DA) cells in standard (CTRL) and bicarbonate-free (HEPES) solution. $E_{IPSP\text{-}A}$ is significantly less hyperpolarized in dopaminergic than in GABAergic neurons under standard conditions. In the absence of bicarbonate, the $E_{IPSP\text{-}A}$ is significantly more positive, and the polarity of $DF_{IPSP\text{-}A}$ is reversed in the dopaminergic neurons. In contrast, there are no significant changes in these parameters in the GABAergic neurons.

The present results revealed substantial KCC2 expression in the vicinity of inhibitory synapses. This is in apparent contrast with our previous study on the hippocampus, in which KCC2 was abundantly expressed close to excitatory synapses (Gulyas et al., 2001). However, it is easy to reconcile these findings on the basis of the assumption that, in both cases, KCC2 is located close to the sites that generate the major Cl^- load. In the hippocampus, the high level of KCC2 close to excitatory synapses was explained on the basis of the likely existence of extrasynaptic high-affinity $GABA_A$ receptors in these subcellular compartments, which would generate a massive electrogenically driven Cl^- influx during synaptic excitation (Gulyas et al., 2001). Nevertheless, as discussed previously (Payne et al., 2003), an intracellular voltage-driven Cl^- load will take place whenever $GABA_A$ receptors are open during postsynaptic excitation, and hence KCC2 expression close to inhibitory synapses in the SNr (or in any brain area for that matter) is not unexpected.

Functional considerations

Cell type-specific differences in the efficacy of intracellular chloride regulation

Because of the substantial depolarizing bicarbonate current mediated by $GABA_A$ receptors, the reversal potential of ionotropic IPSPs in neurons that extrude Cl^- under physiological conditions is significantly more positive than the Cl^- equilibrium potential (Kaila, 1994). After a correction based on the Goldman–Hodgkin–Katz equation (Kaila et al., 1993), assuming a HCO_3^-/Cl^- permeability ratio of 0.2 and an intracellular pH of ~7.1–7.2 ($[HCO_3^-]_i$, ~15 mM), the $E_{IPSP\text{-}A}$ values obtained presently translate to estimates of intraneuronal chloride concentration ($[Cl^-]_i$) of 5 and 8 mM under physiological conditions for nigral GABAergic and dopaminergic neurons, respectively. As could be expected, the absence of neuronal KCC2 expression will lead to a higher $[Cl^-]_i$, which is, indeed, the case with the SNc dopaminergic neurons. Estimates for $[Cl^-]_i$ in the GABAergic neurons and dopaminergic neurons in the absence of bicarbonate yield

values of 5 and 17 mM, respectively, which demonstrates a profound bicarbonate dependence of Cl^- extrusion in the dopaminergic neurons.

Extrusion of Cl^- in SN dopaminergic neurons is most likely achieved by the combined actions of ClC-2, which provides a significant efflux route to cope with an excessive Cl^- load, and of NDAE, which is responsible for the genuinely hyperpolarizing driving force for chloride. Here, it should be emphasized that activation of the NDAE requires an intracellular acid load (Kaila, 1994), and hence this extrusion mechanism cannot maintain a steep hyperpolarizing Cl^- gradient under resting conditions. Furthermore, the transport stoichiometry of the NDAE is based on a 1:2 exchange between Cl^- and acid–base equivalents (Payne et al., 2003), which renders NDAE rather inefficient in terms of Cl^- extrusion even when confronted with an acid load. The present data do not exclude the possibility that the GABAergic cells may also express NDAE. However, even if this is the case, the influence of this transporter on neuronal Cl^- extrusion will be masked by the much more efficient KCC2 cotransporter (see Introduction) (Rivera et al., 1999).

Cell type-specific differences in the efficacy of $GABA_A$ receptor-mediated inhibition

Together, the present observations suggest that one important factor contributing to the higher efficacy of $GABA_A$ receptor-mediated inhibition in GABAergic neurons than in dopaminergic neurons in substantia nigra is the distinct nature of the Cl^- extrusion mechanisms that exist in these cells. $GABA_A$-mediated inhibition appears to be much more effective and stable in the GABAergic neurons (MacNeil et al., 1978; Grace and Bunney, 1979, 1985; Waszczak et al., 1980; Celada et al., 1999), which is consistent with the fact that, unlike the dopaminergic neurons, they are equipped with the highly effective Cl^- extruder KCC2. Our data do not rule out other possible contributing factors such as different subunit compositions of the $GABA_A$ receptors on dopaminergic and GABAergic neurons in substantia nigra (Rodriguez-Pallares et al., 2000; Schwarzer et al., 2001) and/or differences in the density or subcellular location of $GABA_A$ receptors. Nevertheless, the labile nature of ionotropic inhibition in the dopaminergic cells is likely to reflect the fact that the dopaminergic neurons are devoid of KCC2, and that their capability for hyperpolarizing $GABA_A$ receptor-mediated inhibition is strictly dependent on the presence of a bicarbonate-dependent transport mechanism (Fig. 9). In cells of this kind, activity-dependent anion shifts can easily take place, which thereafter could not only lead to a suppression of $GABA_A$-mediated inhibition, but might also produce depolarizing and even functionally excitatory $GABA_A$ receptor-mediated responses (Kaila et al., 1997).

Because a change from inhibitory to excitatory GABAergic transmission is often related to neuronal trauma (van den Pol et al., 1996; Nabekura et al., 2002), an exciting topic in future studies on SNc dopaminergic neurons is the possible relationship between their ionic mechanisms of GABAergic inhibition and their selective vulnerability related to Parkinson's disease.

References

Celada P, Paladini CA, Tepper JM (1999) GABAergic control of rat substantia nigra dopaminergic neurons: role of globus pallidus and substantia nigra pars reticulata. Neuroscience 89:813–825.

DeFazio RA, Keros S, Quick MW, Hablitz JJ (2000) Potassium-coupled chloride cotransport controls intracellular chloride in rat neocortical pyramidal neurons. J Neurosci 20:8069–8076.

Ebihara S, Shirato K, Harata N, Akaike N (1995) Gramicidin-perforated patch recording: GABA response in mammalian neurones with intact intracellular chloride. J Physiol (Lond) 484:77–86.

Enz R, Ross BJ, Cutting GR (1999) Expression of the voltage-gated chloride channel ClC-2 in rod bipolar cells of the rat retina. J Neurosci 19:9841–9847.

Grace AA, Bunney BS (1979) Paradoxical GABA excitation of nigral dopaminergic cells: indirect mediation through reticulata inhibitory neurons. Eur J Pharmacol 59:211–218.

Grace AA, Bunney BS (1985) Opposing effects of striatonigral feedback pathways on midbrain dopamine cell activity. Brain Res 333:271–284.

Grace AA, Onn SP (1989) Morphology and electrophysiological properties of immunocytochemically identified rat dopamine neurons recorded *in vitro*. J Neurosci 9:3463–3481.

Grichtchenko II, Choi I, Zhong X, Bray-Ward P, Russell JM, Boron WF (2001) Cloning, characterization, and chromosomal mapping of a human electroneutral Na^+-driven Cl-HCO_3 exchanger. J Biol Chem 276:8358–8363.

Grofova I (1975) The identification of striatal and pallidal neurons projecting to substantia nigra. An experimental study by means of retrograde axonal transport of horseradish peroxidase. Brain Res 91:286–291.

Gulyas AI, Sik A, Payne JA, Kaila K, Freund TF (2001) The KCl cotransporter, KCC2, is highly expressed in the vicinity of excitatory synapses in the rat hippocampus. Eur J Neurosci 13:2205–2217.

Hebb MO, Robertson HA (2000) Identification of a subpopulation of substantia nigra pars compacta γ-aminobutyric acid neurons that is regulated by basal ganglia activity. J Comp Neurol 416:30–44.

Hontanilla B, Parent A, Gimenez-Amaya JM (1997) Parvalbumin and calbindin D-28k in the entopeduncular nucleus, subthalamic nucleus, and substantia nigra of the rat as revealed by double-immunohistochemical methods. Synapse 25:359–367.

Iribe Y, Moore K, Pang KC, Tepper JM (1999) Subthalamic stimulation-induced synaptic responses in substantia nigra pars compacta dopaminergic neurons *in vitro*. J Neurophysiol 82:925–933.

Isaacs KR, Jacobowitz DM (1994) Mapping of the colocalization of calretinin and tyrosine hydroxylase in the rat substantia nigra and ventral tegmental area. Exp Brain Res 99:34–42.

Jarolimek W, Lewen A, Misgeld U (1999) A furosemide-sensitive K^+–Cl^- cotransporter counteracts intracellular Cl^- accumulation and depletion in cultured rat midbrain neurons. J Neurosci 19:4695–4704.

Javoy-Agid F, Ploska A, Agid Y (1981) Microtopography of tyrosine hydroxylase, glutamic acid decarboxylase, and choline acetyltransferase in the substantia nigra and ventral tegmental area of control and Parkinsonian brains. J Neurochem 37:1218–1227.

Kaila K (1994) Ionic basis of $GABA_A$ receptor channel function in the nervous system. Prog Neurobiol 42:489–537.

Kaila K, Voipio J, Paalasmaa P, Pasternack M, Deisz RA (1993) The role of bicarbonate in $GABA_A$ receptor-mediated IPSPs of rat neocortical neurones. J Physiol (Lond) 464:273–289.

Kaila K, Lamsa K, Smirnov S, Taira T, Voipio J (1997) Long-lasting GABA-mediated depolarization evoked by high-frequency stimulation in pyramidal neurons of rat hippocampal slice is attributable to a network-driven, bicarbonate-dependent K^+ transient. J Neurosci 17:7662–7672.

Kakazu Y, Akaike N, Komiyama S, Nabekura J (1999) Regulation of intracellular chloride by cotransporters in developing lateral superior olive neurons. J Neurosci 19:2843–2851.

Kanaka C, Ohno K, Okabe A, Kuriyama K, Itoh T, Fukuda A, Sato K (2001) The differential expression patterns of messenger RNAs encoding K-Cl cotransporters (KCC1, 2) and Na-K-2Cl cotransporter (NKCC1) in the rat nervous system. Neuroscience 104:933–946.

Kang Y, Kitai ST (1993a) Calcium spike underlying rhythmic firing in dopaminergic neurons of the rat substantia nigra. Neurosci Res 18:195–207.

Kang Y, Kitai ST (1993b) A whole cell patch-clamp study on the pacemaker potential in dopaminergic neurons of rat substantia nigra compacta. Neurosci Res 18:209–221.

Kita T, Kita H, Kitai ST (1986) Electrical membrane properties of rat substantia nigra compacta neurons in an *in vitro* slice preparation. Brain Res 372:21–30.

Lacey MG, Mercuri NB, North RA (1989) Two cell types in rat substantia nigra zona compacta distinguished by membrane properties and the actions of dopamine and opioids. J Neurosci 9:1233–1241.

MacNeil D, Gower M, Szymanska I (1978) Response of dopamine neurons in substantia nigra to muscimol. Brain Res 154:401–403.

McRitchie DA, Hardman CD, Halliday GM (1996) Cytoarchitectural distribution of calcium binding proteins in midbrain dopaminergic regions of rats and humans. J Comp Neurol 364:121–150.

Misgeld U, Deisz RA, Dodt HU, Lux HD (1986) The role of chloride transport in postsynaptic inhibition of hippocampal neurons. Science 232:1413–1415.

Nabekura J, Ueno T, Okabe A, Furuta A, Iwaki T, Shimizu-Okabe C, Fukuda A, Akaike N (2002) Reduction of KCC2 expression and $GABA_A$ receptor-mediated excitation after *in vivo* axonal injury. J Neurosci 22:4412–4417.

Nakanishi H, Kita H, Kitai ST (1987) Intracellular study of rat substantia nigra pars reticulata neurons in an *in vitro* slice preparation: electrical membrane properties and response characteristics to subthalamic stimulation. Brain Res 437:45–55.

Paladini CA, Tepper JM (1999) $GABA_A$ and $GABA_B$ antagonists differentially affect the firing pattern of substantia nigra dopaminergic neurons *in vivo.* Synapse 32:165–176.

Paladini CA, Celada P, Tepper JM (1999) Striatal, pallidal, and pars reticulata evoked inhibition of nigrostriatal dopaminergic neurons is mediated by $GABA_A$ receptors *in vivo.* Neuroscience 89:799–812.

Payne JA, Stevenson TJ, Donaldson LF (1996) Molecular characterization of a putative K-Cl cotransporter in rat brain. A neuronal-specific isoform. J Biol Chem 271:16245–16252.

Payne JA, Rivera C, Voipio J, Kaila K (2003) Cation-chloride co-transporters in neuronal communication, development and trauma. Trends Neurosci 26:199–206.

Precht W, Yoshida M (1971) Blockage of caudate-evoked inhibition of neurons in the substantia nigra by picrotoxin. Brain Res 32:229–233.

Rajakumar N, Elisevich K, Flumerfelt BA (1994) Parvalbumin-containing GABAergic neurons in the basal ganglia output system of the rat. J Comp Neurol 350:324–336.

Ribak CE, Vaughn JE, Saito K, Barber R, Roberts E (1976) Immunocytochemical localization of glutamate decarboxylase in rat substantia nigra. Brain Res 116:287–298.

Richards CD, Shiroyama T, Kitai ST (1997) Electrophysiological and immunocytochemical characterization of GABA and dopamine neurons in the substantia nigra of the rat. Neuroscience 80:545–557.

Rick CE, Lacey MG (1994) Rat substantia nigra pars reticulata neurones are tonically inhibited via $GABA_A$, but not $GABA_B$, receptors *in vitro.* Brain Res 659:133–137.

Rivera C, Voipio J, Payne JA, Ruusuvuori E, Lahtinen H, Lamsa K, Pirvola U, Saarma M, Kaila K (1999) The K^+/Cl^- co-transporter KCC2 renders GABA hyperpolarizing during neuronal maturation. Nature 397:251–255.

Rodriguez-Pallares J, Caruncho HJ, Munoz A, Guerra MJ, Labandeira-Garcia JL (2000) $GABA_A$ receptor subunit expression in intrastriatal ventral mesencephalic transplants. Exp Brain Res 135:331–340.

Romero MF, Henry D, Nelson S, Harte PJ, Dillon AK, Sciortino CM (2000) Cloning and characterization of a Na^+-driven anion exchanger (NDAE1). A new bicarbonate transporter. J Biol Chem 275:24552–24559.

Schwarzer C, Berresheim U, Pirker S, Wieselthaler A, Fuchs K, Sieghart W, Sperk G (2001) Distribution of the major γ-aminobutyric acid(A) receptor subunits in the basal ganglia and associated limbic brain areas of the adult rat. J Comp Neurol 433:526–549.

Schwiening CJ, Boron WF (1994) Regulation of intracellular pH in pyramidal neurones from the rat hippocampus by Na^+-dependent Cl^--HCO_3^- exchange. J Physiol (Lond) 475:59–67.

Sik A, Smith RL, Freund TF (2000) Distribution of chloride channel-2-immunoreactive neuronal and astrocytic processes in the hippocampus. Neuroscience 101:51–65.

Smith Y, Bolam JP (1989) Neurons of the substantia nigra reticulata receive a dense GABA-containing input from the globus pallidus in the rat. Brain Res 493:160–167.

Smith RL, Clayton GH, Wilcox CL, Escudero KW, Staley KJ (1995) Differential expression of an inwardly rectifying chloride conductance in rat brain neurons: a potential mechanism for cell-specific modulation of postsynaptic inhibition. J Neurosci 15:4057–4067.

Staley K (1994) The role of an inwardly rectifying chloride conductance in postsynaptic inhibition. J Neurophysiol 72:273–284.

Tepper JM, Martin LP, Anderson DR (1995) $GABA_A$ receptor-mediated inhibition of rat substantia nigra dopaminergic neurons by pars reticulata projection neurons. J Neurosci 15:3092–3103.

van den Pol AN, Obrietan K, Chen G (1996) Excitatory actions of GABA after neuronal trauma. J Neurosci 16:4283–4292.

Vardi N, Zhang LL, Payne JA, Sterling P (2000) Evidence that different cation chloride cotransporters in retinal neurons allow opposite responses to GABA. J Neurosci 20:7657–7663.

Vu TQ, Payne JA, Copenhagen DR (2000) Localization and developmental expression patterns of the neuronal K-Cl cotransporter (KCC2) in the rat retina. J Neurosci 20:1414–1423.

Waszczak BL, Eng N, Walters JR (1980) Effects of muscimol and picrotoxin on single unit activity of substantia nigra neurons. Brain Res 188:185–197.

Williams JR, Sharp JW, Kumari VG, Wilson M, Payne JA (1999) The neuron-specific K-Cl cotransporter, KCC2. Antibody development and initial characterization of the protein. J Biol Chem 274:12656–12664.

Wilson CJ, Callaway JC (2000) Coupled oscillator model of the dopaminergic neuron of the substantia nigra. J Neurophysiol 83:3084–3100.

Ye J (2000) Physiology and pharmacology of native glycine receptors in developing rat ventral tegmental area neurons. Brain Res 862:74–82.